Brain Pathology ISSN 1015–6305

RESEARCH ARTICLE

Altered Machinery of Protein Synthesis in Alzheimer's: From the Nucleolus to the Ribosome

Karina Hernández-Ortega[1,2]; Paula Garcia-Esparcia[1,2]; Laura Gil[3]; José J. Lucas[2,4]; Isidre Ferrer[1,2]

[1] Institute of Neuropathology, Service of Pathologic Anatomy, IDIBELL-Bellvitge University Hospital, University of Barcelona, Hospitalet de Llobregat, Spain.
[2] Neuropathology, CIBERNED (Centro de Investigación Biomédica en Red de Enfermedades Neurodegenerativas), Madrid, Spain.
[3] Department of Genetics, Medical School, Alfonso X el Sabio University (UAX), Villanueva de la Cañada; Centro de Investigaciones Biologicas (CIB), CSIC, Madrid, Spain.
[4] Department of Molecular Biology, Center for Molecular Biology "Severo Ochoa" (CBMSO) CSIC/UAM, Madrid, 28049, Spain.

Keywords
Alzheimer's disease, elongation factors of protein synthesis, histones, initiation factors, nuclear tau, nucleolin, nucleolus, nucleophosmin, nucleoplasmin, nucleus, protein synthesis, ribosome, ribosomal proteins, upstream binding transcription factor RNA polymerase I.

Corresponding author:
Isidre Ferrer, MD, PhD, Institute of Neuropathology, Service of Pathologic Anatomy, Bellvitge University Hospital, carrer Feixa Llarga s/n, 08907 Hospitalet de Llobregat, Spain (E-mail: *8082ifa@gmail.com*)

Received 12 July 2015
Accepted 22 October 2015
Published Online Article Accepted 29 October 2015

The authors declare that they have no disclosures or conflicts of interest.

doi:10.1111/bpa.12335

Abstract

Ribosomes and protein synthesis have been reported to be altered in the cerebral cortex at advanced stages of Alzheimer's disease (AD). Modifications in the hippocampus with disease progression have not been assessed. Sixty-seven cases including middle-aged (MA) and AD stages I–VI were analyzed. Nucleolar chaperones nucleolin, nucleophosmin and nucleoplasmin 3, and upstream binding transcription factor RNA polymerase I gene (*UBTF*) mRNAs are abnormally regulated and their protein levels reduced in AD. Histone modifications dimethylated histone H3K9 (H3K9me2) and acetylated histone H3K12 (H3K12ac) are decreased in CA1. Nuclear tau declines in CA1 and dentate gyrus (DG), and practically disappears in neurons with neurofibrillary tangles. Subunit 28 ribosomal RNA (28S rRNA) expression is altered in CA1 and DG in AD. Several genes encoding ribosomal proteins are abnormally regulated and protein levels of translation initiation factors eIF2α, eIF3η and eIF5, and elongation factor eEF2, are altered in the CA1 region in AD. These findings show alterations in the protein synthesis machinery in AD involving the nucleolus, nucleus and ribosomes in the hippocampus in AD some of them starting at first stages (I–II) preceding neuron loss. These changes may lie behind reduced numbers of dendritic branches and reduced synapses of CA1 and DG neurons which cause hippocampal atrophy.

INTRODUCTION

Alzheimer's disease (AD) is characterized clinically by progressive loss of memory and cognitive decline leading to dementia, and histophalogicaly by atrophy of the brain typically involving the hippocampus and medial region of the temporal lobes even at early stages of the disease. The neuropathological markers are on one hand, phosphorylated and truncated tau that deposit in the form of neurofibrillary tangles (NFTs), neuropil threads and plaque-surrounding dystrophic neurites and, on the other hand, extracellular β-amyloid that deposits in the form of diffuse and neuritic or senile plaques, and in the walls of blood vessels. At initial asymptomatic stages, NFTs in the cerebrum are restricted to the transentorhinal and entorhinal cortices and CA1 region of the hippocampus. Later on, NFTs spread to the amygdala, and nuclei of the forebrain and the whole neocortex, among other areas. Although following a distinct pattern, β-amyloid deposits also spread from the basal regions of the cerebrum to cover practically the entire telencephalon (10). Examination of large series of post-mortem brains has shown that AD-related pathology, at least at stages I-II and III of Braak and Braak, occurs in about 80% of individuals aged 65 years, while only about 5% have the extensive lesions that correspond to stages IV, V or VI and manifest cognitive impairment and dementia (11–13, 35). Progression of NFTs and plaques accompanied by cerebral atrophy is causative of severe cognitive impairment and dementia in about 25% of human beings aged 80 years. Therefore, AD is a progressive neurodegenerative process developing over many years and not necessarily leading to dementia (35). The silent period, if properly detected, would permit the administration of therapies geared to curbing disease progression before the magnitude of nerve tissue damage is too extensive. One of the most commonly used markers to verify disease progression is neuroimaging examination of the hippocampal formation to detect early atrophy in this region (3, 5, 8, 16, 20, 23, 54, 63).

Hippocampal atrophy in AD has been interpreted as secondary to neurofibrillary tangle formation, neuron atrophy and loss of neurons. However, the cause of neuron atrophy has not been examined in detail although one of the most plausible causes is reduced protein synthesis. Seminal studies identified altered composition of

Table 1. mRNA expression of nucleolar proteins and 18S rRNA and 28S rRNA in the DG and CA1 region of the hippocampus of MA and AD cases.

Probe	MA	AD I–II	AD III–IV	AD V–VI	MA vs. AD I–II	MA vs. AD III–IV	MA vs. AD V–VI
DG							
NCL	1.01 ± 0.18	1.19 ± 0,19	0.98 ± 0,23	0.91 ± 0.26	NS	NS	NS
NPM1	1.01 ± 0.17	1.07 ± 0.22	1.01 ± 0.22	0.67 ± 0.20	NS	NS	**↓
NPM3	1.17 ± 0.19	0.91 ± 0.14	0.99 ± 0.15	0.64 ± 0.09	NS	NS	*↓
UBTF	1.02 ± 0.22	0.76 ± 0.25	0.81 ± 0.19	0.25 ± 0.08	NS	NS	***↓
CA1							
NCL	1.04 ± 0.30	1.22 ± 0.12	1.09 ± 0.37	0.58 ± 0.20	NS	NS	**↓
NPM1	1.02 ± 0.25	1.36 ± 0.12	1.35 ± 0.17	1.04 ± 0.30	*↑	*↑	NS
NPM3	1.06 ± 0.10	1.09 ± 0.10	1.49 ± 0.15	0.57 ± 0.07	NS	*↑	**↓
UBTF	1.05 ± 0.35	0.54 ± 0.14	0.60 ± 0.13	0.59 ± 0.16	***↓	**↓	**↓
DG							
18S rRNA	1.04 ± 0.34	0.74 ± 0.11	0.80 ± 0.40	1.13 ± 0.22	NS	NS	NS
28S rRNA	1.10 ± 0.52	0.66 ± 0.17	0.47 ± 0.19	1.90 ± 0.63	NS	**↓	NS
CA1							
18S rRNA	1.10 ± 0.45	0.65 ± 0.36	1.13 ± 0.11	1.51 ± 0.31	NS	NS	NS
28S rRNA	1.15 ± 0.67	0.45 ± 0.19	0.43 ± 0.22	2.65 ± 0.85	*↓	*↓	**↑

Expression levels are calculated using Gus-β for normalization; Student *t*-test *$P < 0.05$; **$P < 0.01$; ***$P < 0.001$ compared with MA.

ribosomes and abnormal expression levels of certain transcription factors, and impaired protein synthesis in cortical areas in cases with mild cognitive impairment and dementia caused by AD (26, 34, 62, 64, 84). The main modifications were reduced rRNA levels, increased RNA oxidation as shown by increased 8-hydroxyguanosine immunoreactivity, and reduced capacity of isolated polyribosomes to incorporate S^{35} methionine into protein (26, 27, 48, 75, 76, 90, 91). Moreover, the nuclear organizer region (NOR) surface/total nucleus surface is reduced (22, 28), and the rDNA promoter is hyper-methylated in AD, thus suggesting epigenetic silencing of rDNA at very precise times of AD progression (80). Together, these findings suggest a complex scenario in which several pathways, from the nucleus and nucleolus to the ribosome, are altered in the cerebral cortex in AD.

This study analyzes expression of mRNAs of genes playing an important role in nucleolar function and rRNA biosynthesis, protein levels and localization, rRNA levels, mRNA expression of several ribosomal proteins, expression of selected histones involved in nucleolar processing, and expression levels of initiation and elongation factors of protein synthesis in the CA1 region and dentate gyrus (DG) of the hippocampus in middle-aged individuals (MA) and AD cases stages I–II, III–IV and V–VI. The aim of the study was to assess in parallel in the same cases, (i) possible alterations of the pathways involved in protein synthesis; (ii) changes at very early stages of the disease in which changes cannot be attributed to neuron loss in comparison with changes observed at advanced stages of the disease; and (iii) possible differences in the CA1 region and the DG, the first one with development of NFTs and the second without, but both affected by reduced dendritic branches and loss of spines with AD progression.

MATERIAL AND METHODS

Tissue samples

Brain samples were obtained from the Institute of Neuropathology HUB-ICO-IDIBELL Biobank following European Union legislation and the approval of the local ethics committee. The time from death to tissue processing (post-mortem delay) was between 3 and 18 h. At autopsy, one hemisphere was rapidly cut in coronal sections 1-cm thick and selected areas of the encephalon were dissected, frozen on dry ice, and stored at −80°C into labeled plastic bags until use. The other hemisphere was fixed by immersion in 4% buffered formalin for 3 weeks for morphologic examination. Neuropathological study was performed on 25 regions of the cerebral cortex, diencephalon, thalamus, brainstem and cerebellum. Dewaxed paraffin sections were stained with haematoxylin and eosin and Klüver-Barrera, and processed for immunohistochemistry to microglia specific markers, glial fibrillary acidic protein, β-amyloid, phosphorylated tau, α-synuclein, TDP-43, ubiquitin and p62. Neuropathological diagnosis of AD was performed following the Braak and Braak stages (10, 12) adapted to paraffin sections (9).

The AD cases included in the present study were 16 stages I–II (4 women, 12 men), 16 stages III–IV (9 women, 7 men) and 17 stages V–VI (9 women, 8 men). Cases with additional pathologies, including Lewy body diseases, tauopathies (particularly argyrophilic grain disease), vascular diseases, TDP-43pathies, and metabolic syndrome were excluded. MA cases ($n = 18$) had not suffered from neurologic or psychiatric diseases, and did not have lesions in the neuropathological study (including vascular, hypoxic, and inflammatory). Two regions, CA1 region and the DG, were examined in parallel. For biochemical studies, these regions were dissected separately under a low magnification microscope, whereas the total hippocampal complex, part of the entorhinal cortex, and the lower temporal gyrus were included in the same bloc for morphological studies. A summary of the cases analyzed is shown in Supporting Information Table I.

RNA purification

Total RNA of the CA1 and DG was isolated using the RNeasy Lipid Tissue Mini Kit (Qiagen, Hilden, Germany) according to the protocol of the supplier. Samples were treated with RNase-free DNase Set (Qiagen) for 15 minutes to avoid extraction and later

amplification of genomic DNA. The RNA concentration of each sample was measured at *A*260 nm using a NanoDrop 2000 spectrophotometer (Thermo-Scientific, Waltham, MA, USA). RNA integrity number (RIN) was calculated using the Agilent 2100 Bioanalyzer (Agilent, Santa Clara, CA, USA). The RIN values of the samples varied from 6.3 to 7.9.

cDNA synthesis

The reverse transcription reaction of RNA was performed with the High-Capacity cDNA Archive kit (Applied Biosystems, Foster City, CA, USA) following the manufacturer's guidelines and using a Gene Amp 9700 PCR System thermo-cycler (Applied Biosystems). To test for the presence of contaminating DNA, a parallel reaction in one RNA sample was run in the absence of reverse transcriptase.

TaqMan PCR

Samples analyzed with TaqMan polymerase chain reaction (PCR) comprised 14 controls (7 women, 7 men) and 28 AD cases (14 women, 14 men) (Table 1). TaqMan PCR assays were performed on 384 optical plates utilizing the ABI Prism 7900 HT Sequence Detection System (Applied Biosystems). The cDNA samples obtained from the retro-transcription reaction were diluted 1:20, and TaqMan PCR assays for each gene were performedin duplicate. For each TaqMan reaction, 9 μL of cDNA was mixed with 1 μL 20X TaqMan Gene Expression Assay and 10 μL of 2X TaqMan Universal PCR Master Mix (Applied Biosystems). The reactions were performed as follows: 50°C for 2 minutes, 95°C for 10 minutes and 40 cycles at 95°C for 15 s and 60°C for 1 minutes. TaqMan PCR data were captured using the Sequence Detection Software (SDS version 2.2, Applied Biosystems). TaqMan probes used in the study are shown in Supporting Information Table II. Parallel assays for each sample were performed using TaqMan probes for β-glucuronidase (*GUS-β*) and X-prolyl aminopepidase P1 (*XPNPEP1*) as endogenous controls.

For the data analysis, threshold cycle (CT) values for each sample were processed to obtain double delta CT (ΔΔCT) values. First, delta CT (ΔCT) values were calculated as the normalized CT values for each target gene in relation to the CT of endogenous controls GUS-β and XPNPEP1. Then, ΔΔCT values were obtained from the ΔCT of each sample minus the mean ΔCT of the population of control samples (calibrator samples). The fold change was calculated using the equation $2^{(-\Delta\Delta CT)}$. Mean fold-change values for each region and experimental group were analyzed with Student-*t* test using the Graph Pad Prism 5 Software. Differences between AD stages and MA group were considered statistically significant at $*P < 0.05$, $**P < 0.01$, and $***P < 0.001$.

Immunohistochemistry

Inmunohistochemical assessment was performed on 4-μm-thick dewaxed paraffin sections obtained with a sliding microtome. The sections were boiled in citrate buffer (10 mM sodium citrate, pH 6.0) for 20 minutes to retrieve antigens and then washed with PBS. Then, endogenous peroxidases were blocked with Dako Peroxidase Blocking Reagent (DAKO, Glostrup, Denmark) for 10 minutes. Primary antibodies were diluted in Dako Antibody Diluent (DAKO Corporation, USA) and incubated overnight at 4°C (see Supporting Information Table III for details). After incubation with the primary antibody and PBS rinses, sections were incubated at room temperature with the Super Sensitive^{TM} link-label IHC Detection System (Biogenex, Fremont, CA, USA) according to the manufacturer's instructions. The peroxidase reaction was visualized with 3′3-diaminobenzidine (Liquid DAB+ Substrate Chromogen System, DAKO Corporation, USA). Finally, the sections were dehydrated and cover-slipped for microscopic observation. To test the specificity of immunoreaction some sections were incubated without the primary antibodies; the staining was negative.

Cell counting

Histological sections were captured with a ProgRes camera (Jenoptik, Germany) attached to a Nikon Eclipse E800 microscope (Tokyo, Japan). Cell counting was performed on 4-μm-thick sections corresponding to DG and CA1, from four to six cases per group. The number of positive cells for different markers was recorded in three optical fields at 400X magnification. Mean data were analyzed with one-way ANOVA followed by Tukey's test *post hoc* analysis. Statistical examination was performed in Graph Pad Prism 5. Differences between MA and AD groups were considered significant at $*P < 0.05$, $**P < 0.01$ and $***P < 0.001$.

Western blotting

Tissue samples of CA1 (0.1 g) were homogenized in 1 mL of Mila lysis buffer (100 mM Tris/HCl buffer pH 7.4, containing 100 mM NaCl, 10 mM ethylenediaminetetraacetate (EDTA), 0.5% sodium deoxycholate, 0.5% Nonidet-P40, and protease and phosphatase inhibitor cocktails), and then centrifuged at 4°C for 10 minutes at 5000 rpm. The protein content was quantified with the Bradford method. Afterwards, 20 μg of protein was loaded into a 12% SDS-PAGE and then electrophoresis proteins were transferred to nitrocellulose membranes. Membranes were blocked with TBS containing 5% non-fat dry milk and 0.1% Tween 20 for 1 h at room temperature and then incubated overnight at 4°C with the appropriate primary antibody (Table 3). After washing with TBS/0.1%Tween 20, the membranes were incubated for 1 h at room temperature with the corresponding horseradish peroxidase-conjugated secondary anti-body (1:2000; Dako) (Table 3), and the immune complexes were detected by chemiluminescence (ECL, Amersham, Fairfield, CT, USA). The densitometric analysis of western blot bands was conducted using the NIH ImageJ software (Bethesda, MD, USA). Densitometric protein values were normalized with β-actin levels and expressed as an optical density ratio. Statistical differences between MA and AD groups were analyzed with one-way analysis of variance (ANOVA) followed by Tukey's test *post hoc* analysis. Statistical examination was performed in Graph Pad Prism 5. Differences were considered significant at $*P < 0.05$, $**P < 0.01$ and $***P < 0.001$.

RESULTS

Changes in mRNA expression and protein levels of nucleolar genes in DG and CA1 of AD

No modifications in the mRNA expression levels of nucleolin (*NCL*), nucleophosmin (*NPM1*), nucleoplasmin 3 (*NPM3*) and upstream binding transcription factor, RNA polymerase I (*UBTF*) were observed in the DG of AD cases at stages I–II and III–IV when compared with MA. However, significantly reduced

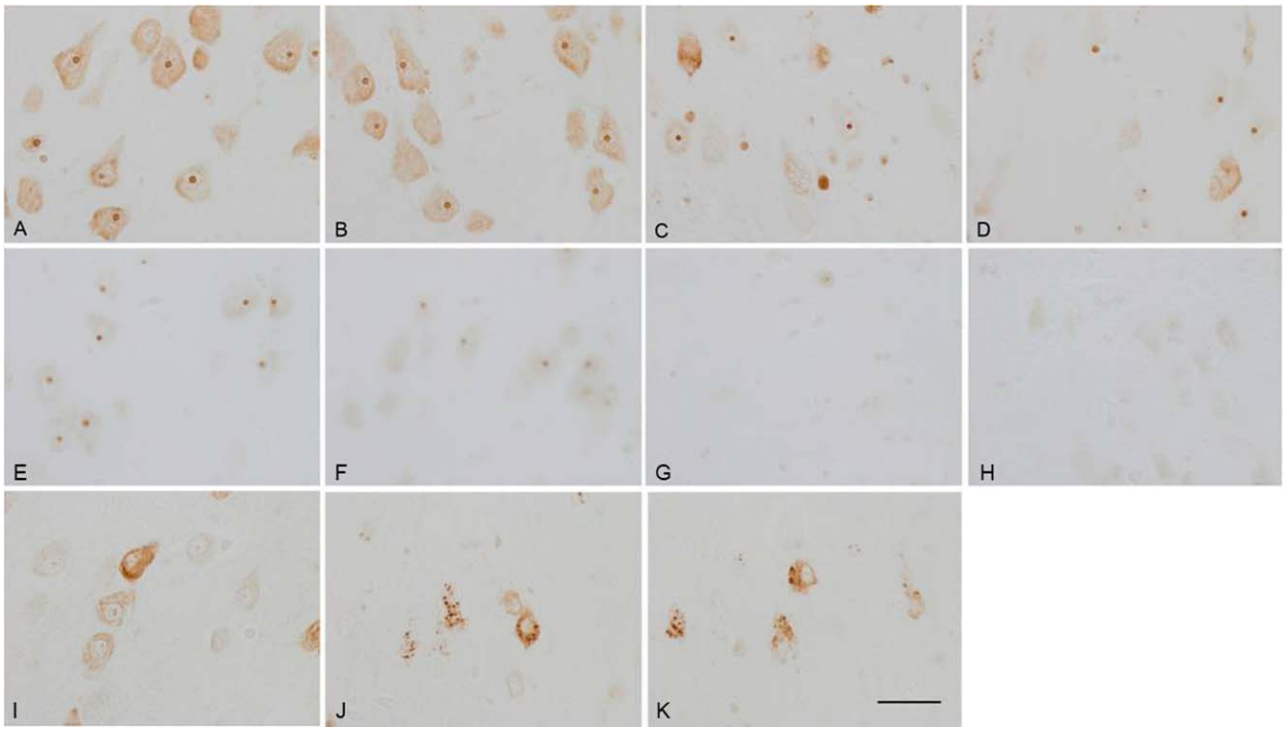

Figure 1. *NPM1, NPM3 and NCL in MA cases and AD at different stages of disease progression*. **A–D.** NPM1/B23 in CA1 (A–D), in MA (A) and AD cases stages I–II (B), III–IV (C) and V–VI (D). **E–H.** NPM3 in the CA1 region of the hippocampus in MA (E), AD stage I-II (F), IV (G) and V (H) of Braak and Braak. **I–K.** Nucleolin in CA1 in MA (I) and AD stage V–VI (J, K). Decreased numbers of nucleoli and reduced nucleolar NPM1, NPM3 and NCL immunoreactivity in remaining nucleoli is observed in neurons at stages III–IV and V–VI when compared with MA and AD cases stages I–II. A few CA1 neurons show, in addition to weak nucleolar staining, NCL immunoreactivity. Cytoplasmic granules in neurons with granulovacuolar degeneration are strongly NCL immunoreactive. Paraffin sections without haematoxylin counterstaining permit a perfect visualization of the nucleolus, bar = 25 μm.

expression of NPM1, NPM3 and *UBTF* mRNAs was seen in the DG of AD cases at stages V–VI (Table 1).

Regarding the CA1 region, NPM1 up-regulation and *UBTF* down-regulation were observed in AD at stages I–II and III–IV when compared with MA cases. In addition, *NPM3* mRNA was up-regulated at stages III–IV (Table 1). This was followed by significantly reduced expression of *NCL, NPM3* and *UBTF* mRNAs, and normal *NPM1* mRNA levels at stages V–VI (Table 1).

Immunohistochemistry further revealed alterations in level and distribution of nucleolar proteins with disease progression. NPM1 antibodies decorated the nucleolus of CA1 neurons in MA individuals but NPM1 immunoreactivity decreased in the nucleolus of CA1 neurons along disease progression, with the immunostaining being very weak at stages V–VI (Figure 1A–D). NPM1 immunoreactivity also decreased in DG. A nucleolar pattern was also observed for NPM3 in CA1 and DG. NPM3 immunoreactivity progressively faded in the nucleolus of CA1 and DG neurons with disease progression (Figure 1E–H). NCL immunohistochemistry revealed a particular pattern in MA brains, in addition to the weak nucleolar immunostaining, a few CA1 neurons showed cytoplasmic immunoreactivity. Decreased nucleolar immunostaining in CA1 neurons with disease progression was also observed for NCL. Curiously, NCL was localized in cytoplasmic granules recognized as granulovacuolar degeneration in CA1 neurons at advanced stages of AD (Figure 1I–K).

UBF (the product encoded by *UBTF*) immunoreactivity was observed in the nucleolus of CA1 neurons and of neurons of the entorhinal cortex and inner temporal neocortex, but it was dispersed in the nucleus of the DG granule cells in MA individuals (Figure 2A–D). Nucleolar and diffuse nuclear UBF immunoreactivity decreased with AD progression (Figure 2E–L). In addition, UBF immunoreactivity translocated to the cytoplasm and was integrated into NFTs but not in dystrophic neurites of senile plaques (Figure 2E–L).

Considering the total number of nucleoli in a particular section those stained with Nissl stain, quantification of stained nuclei with antibodies anti-NPM1, NPM3, NCL and UBF revealed a significant decrease (ranging from $P < 0.05$ to $P < 0.001$) in the immunoreactivity of all these markers in CA1 and DG with AD progression. Quantitative values of these changes at different stages of AD are shown in Table 2.

Importantly, no immunohischemical differences regarding NPM1, NPM3, NCL and UBF were seen between MA individuals and AD cases at stages I–II in DG and CA1. However, reduced numbers of nucleoli, as revealed with Nissl stain, and reduced numbers of NPM1, NPM3, NCL and UBF-immunoreactive nucleoli was observed in CA1 at stages III–IV, and more markedly at stages V–VI (Table 2). A similar pattern, although less severe, was seen in DG (Table 2). Detailed inspection of figures revealed that, in addition to reduced numbers of immunoreactive nucleoli,

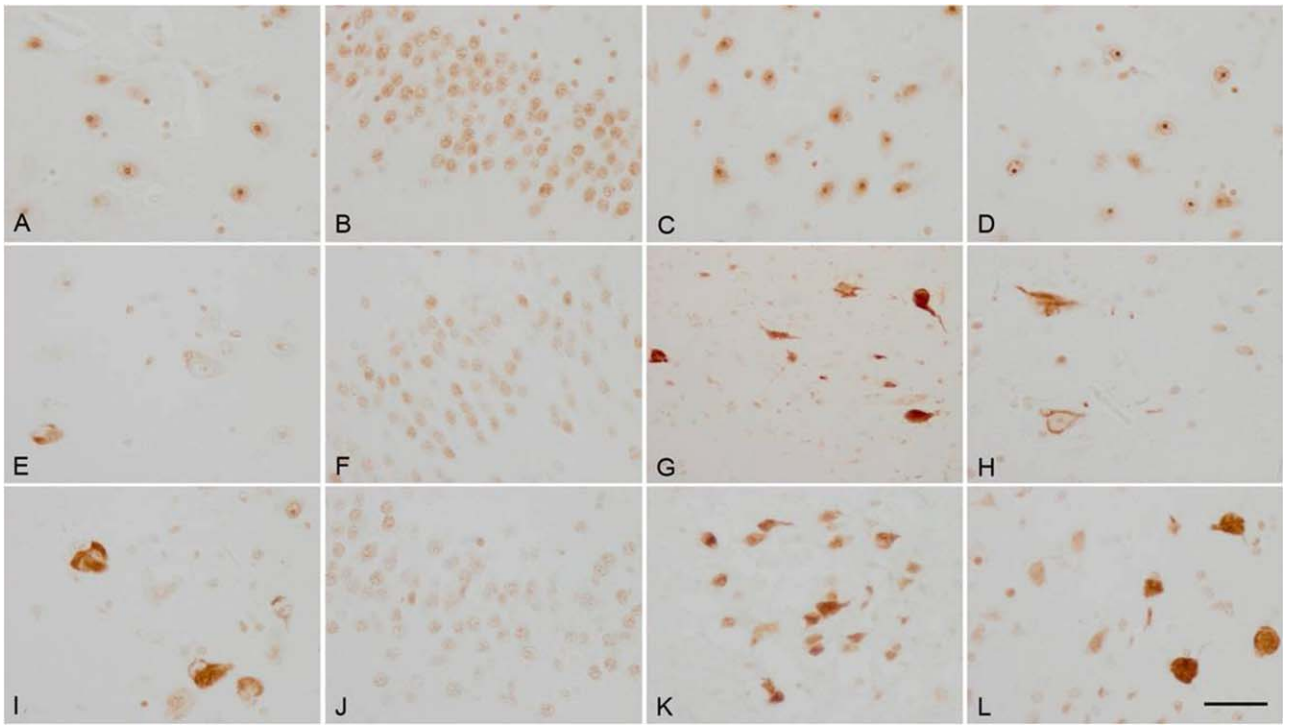

Figure 2. *UBF in MA cases and AD at different stages of disease progression*. **A–D.** MA; **E–H.** AD stage III–IV; **I–L.** AD stage V–VI of Braak and Braak. A, E, I: CA1 region of the hippocampus; B, F, J: dentate gyrus; C, G, K: entorhinal cortex; D, H, L: temporal cortex. UBF-immunoreactive nucleoli decrease and UBF nucleolar immunostaining fades at staged III–IV and V–VI when compared with MA cases. This is particularly evident in neurons bearing NFTs. Moreover UBF immunoreactivity locates to the cytoplasm and decorates NFTs. Paraffin sections without haematoxylin counterstaining, bar = 25 μm.

Table 2. Quantification of nucleoli in CA1 and DG in MA and AD at different stages of disease progression as revealed with Nissl staining and with NPM1, NPM3, NCL and UBF immunohistochemistry. Quantification of positive nuclei as revealed with antibodies anti-H3K9me2, H4K12ac and tau-100.

Marker	MA	AD I–II	AD III–IV	AD V–VI	MA vs. AD I–II	MA vs. AD III–IV	MA vs. AD V–VI
DG							
Nissl	108.28 ± 1.07	104.33 ± 0.85	101.17 ± 1.01	95.83 ± 1.28	NS	*↓	***↓
NPM1	109.00 ± 3.40	107.67 ± 3.37	98.33 ± 3.28	94.42 ± 2.87	NS	NS	* ↓
NPM3	115.34 ± 2.95	110.59 ± 2.20	102.67 ± 2.51	93.08 ± 2.30	NS	**↓	***↓
NCL	116.50 ± 1.84	115.75 ± 1.71	108.67 ± 1.37	100.33 ± 2.93	NS	NS	**↓
UBF	115.33 ± 2.91	106.89 ± 1.55	98.00 ± 3.29	91.00 ± 2.24	NS	**↓	***↓
tau-100	114.30 ± 1.18	108.50 ± 2.47	102.60 ± 1.70	94.13 ± 2.16	NS	*↓	***↓
H3K9me2	109.88 ± 2.33	100.92 ± 0.71	93.50 ± 1.52	87.25 ± 1.57	*↓	***↓	***↓
H4K12ac	111.13 ± 1.20	107.58 ± 1.71	97.04 ± 2.12	89.58 ± 1.20	NS	***↓	***↓
CA1							
Nissl	36.96 ± 1.04	34.30 ± 0.75	31.28 ± 1.30	27.92 ± 1.08	NS	*↓	**↓
NPM1	40.88 ± 0.86	38.29 ± 1.56	33.94 ± 1.60	27.63 ± 0.95	NS	*↓	***↓
NPM3	40.50 ± 1.10	39.25 ± 1.17	35.08 ± 1.36	27.58 ± 1.21	NS	*↓	***↓
NCL	41.17 ± 0.87	38.58 ± 0.76	33.42 ± 1.52	28.89 ± 0.78	NS	**↓	***↓
UBF	39.22 ± 1.06	37.17 ± 1.16	31.11 ± 0.97	26.27 ± 0.48	NS	**↓	***↓
tau-100	41.92 ± 1.08	36.63 ± 0.98	30.17 ± 1.09	27.28 ± 1.01	NS	***↓	***↓
H3K9me2	38.13 ± 1.33	32.33 ± 0.89	29.28 ± 0.72	26.75 ± 0.89	*↓	***↓	***↓
H4K12ac	39.00 ± 1.08	36.30 ± 0.78	30.50 ± 1.06	28.04 ± 0.53	NS	***↓	***↓

Data are expressed as the mean ± Standard error of the mean (SEM) of four to six cases per group; one-way ANOVA followed by Tukey's test *post hoc* analysis *$P < 0.05$, **$P < 0.01$, ***$P < 0.001$.

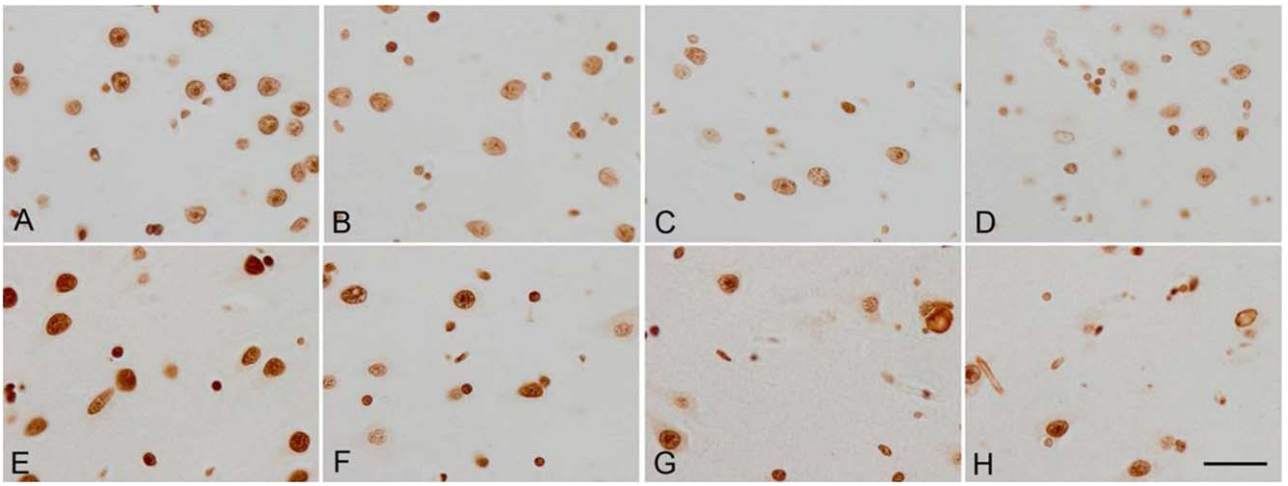

Figure 3. *Histone modifications in AD.* **A–D.** H3K9m2, **E–H.** H4K12ac; CA1 region of the hippocampus. A, E: MA individuals; AD stages I–II (B), III–IV (C, F) and V–VI (D, G, H). Individual selective loss of nuclear neuronal immunoreactivity and rare formation of H4K12ac-immunoreactive globules and bars at advanced stages of AD. Paraffin sections without haematoxylin counterstaining, bar = 25 μm

individual remaining nucleoli showed reduced immunoreactivity at AD stages III–IV and V–VI (Figure 1).

Modifications of histones and nuclear tau in DG and CA1 in AD

NCL and NPMs regulate rRNA transcription through the modulation of histone modifications dimethylated histone H3K9 (H3K9me2) and acetylated histone H3K12 (H3K12ac) in rRNA genes (18, 98). To learn whether NCL and NPM3 changes were associated to modifications in histone methylation and acetylation in AD, immunohistochemistry to specific methylated and acetylated sites in those histones was performed in the same samples. H3K9me2 (Figure 3A–D) and H4K12ac (Figure 3E–H) staining declined in CA1 and DG neurons with disease progression (Table 2). Moreover, H4K12ac-immunoreactive globules and bars in the neuropil of the hippocampus were noted at advanced stages of AD (Figure 3G,H).

Non-phosphorylated tau is present at the internal periphery of nucleoli and the nucleus (87). Accordingly, tau-100 antibody stained the nuclei of neurons and glial cells of CA1, DG, hilus, entorhinal cortex and temporal cortex in MA brains (Figure 4A,E,I,M,O). Decreased tau-100 nuclear immunoreactivity was observed in all these regions in AD with disease progression. This was accompanied by translocated tau-100 immunoreactivity to NFTs and dystrophic neurites of senile plaques in CA1, entorhinal cortex and temporal neocortex (Figure 4A–P). Interestingly, although nuclear tau-100 immunoreactivity was reduced in all these regions, only total disappearance of tau-100 in the nucleus paralleled cytoplasmic tau accumulation in NFTs (Figure 4C,D,L,N,P). Quantitative data are shown in Table 2.

rRNAs in DG and CA1 of AD

Subunit 18 ribosomal RNA (18S rRNA) was not significantly altered in the DG in AD when compared with MA cases. However, subunit 28 ribosomal RNA (28S rRNA) was down-regulated in the DG in AD stages III-IV in relation to MA cases. Regarding CA1, no modifications in 18S rRNA expression levels were found at any stage; 28S rRNA was reduced in AD I–II and AD III–IV but it was found to be up-regulated at AD stages V–VI compared with MA (Table 1).

mRNA expression of ribosomal proteins in DG and CA1 of AD

mRNA levels of *RPL23A*, *RPL26*, *RPL31*, *RPS5*, *RPS6*, *RPS10* and *RPS13* were down-regulated in the DG in AD I–II compared with MA; and mRNAs of *RPL21*, *RPL23A*, *RPL27*, *RPS5*, *RPS6*, *RPS10*, and *RPS13* in AD III–IV in comparison with MA. *RPL7*, *RPL21*, *RPL26*, *RPL27*, *RPL31*, *RPS10*, *RPS16* and *RPS17* mRNA levels were significantly down-regulated and *RPL22* up-regulated in DG at stages V–VI when compared with MA cases (Table 3).

Regarding CA1, *RPL5* and *RPL26* mRNAs were up-regulated and *RPS5* and *RPS26* mRNAs down-regulated in AD I-II in relation to MA cases. *RPL5* mRNA was up-regulated and *RPL23A* and *RPS5* down-regulated at stages II–IV. *RPL5* and *RPL30* mRNAs were up-regulated at stages V–VI, but *RPL21*, *RPL23A*, *RPL26*, *RPL31*, *RPS6*, *RPS10*, *RPS13*, *RPS16* and *RPS17* significantly down-regulated at stages V–VI (Table 3).

Translation initiation and elongation factors in CA1 of AD

Western blotting was used to assess the protein levels of initiation factors eIF2α, eIF3η, and eIF5 and elongation factors eEF1A and eEF2 in the CA1 region in MA and AD cases at different stages of disease progression. The small size of the DG did not permit the use of available frozen samples for these protein studies.

Increased eIF2α protein levels were found at stages III–IV and V–VI, whereas decreased expression of eIF3η occurred in parallel at the same stages of AD. A slight reduction in eIF5 was found only at stages III–IV (Figure 5A).

Reduced eEF2 protein levels were identified only at stages I–II and normalized thereafter. No modifications in the expression levels of eEF1A were noted with disease progression (Figure 5B).

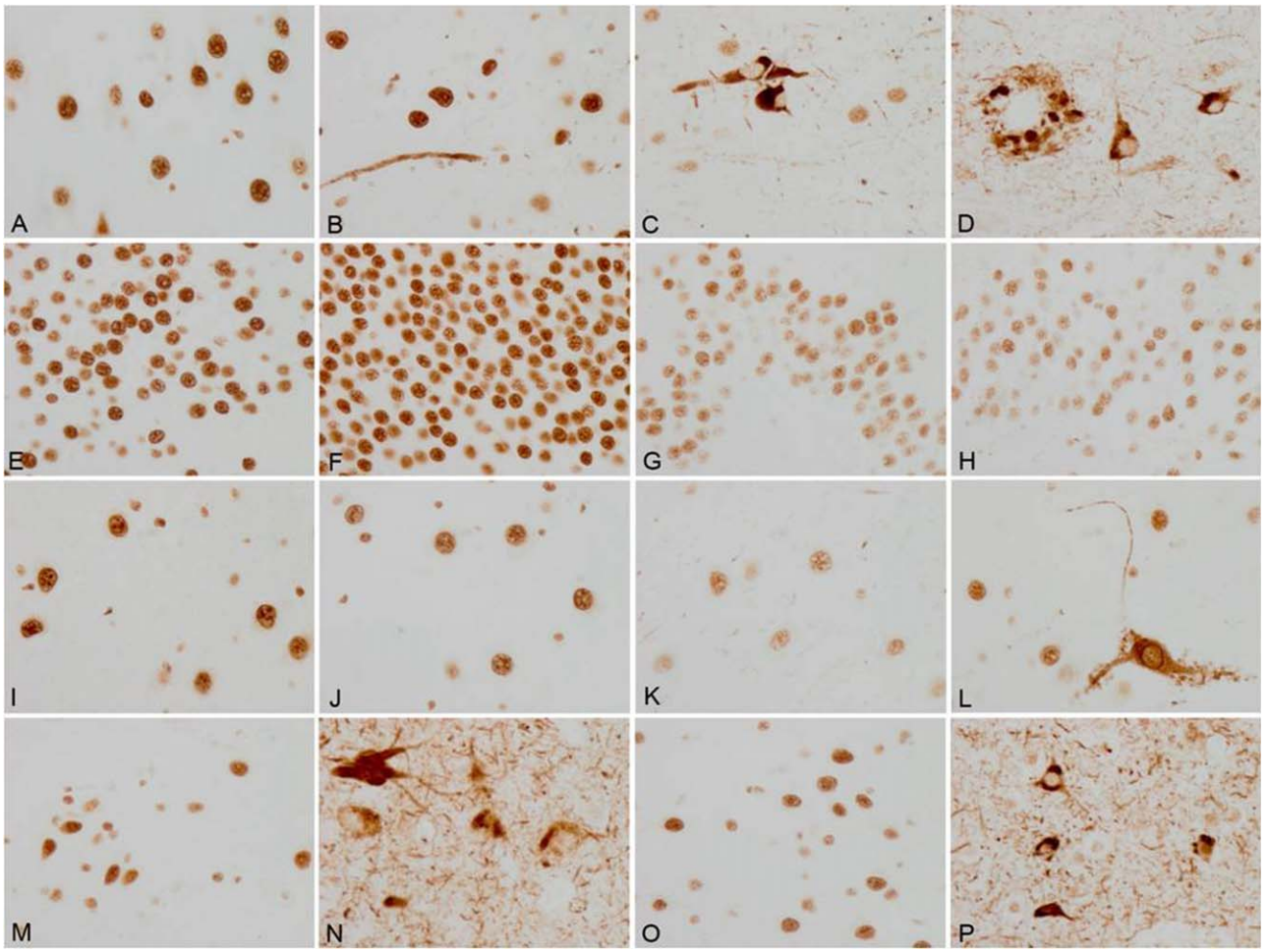

Figure 4. *Tau-100 immunohistochemistry.* **A–D.** CA1 region of the hippocampus; **E–H.** dentate gyrus; **I–L.** hilus; **M, N.** entorhinal cortex; **O, P.** temporal cortex layer V. A, E, I, M: Middle-aged (MA); B, F, J: AD stage II of Braak and Braak; C, G, K, N: stage III of Braak; D, H, L, P: stage V. Tau-100 immunoreactivity is present in the nucleus of neurons and glial cells in MA brains. Decreased tau-100 nuclear immunoreactivity occurs in AD with disease progression. Almost complete absence of tau-100 immunoreactivity in the nucleus is seen in neurons with NFTs in CA1, entorhinal cortex, and temporal neocortex. Note that reduced nuclear tau-100 immunoreactivity is not necessarily accompanied by NFT formation. Tau-100 also decorates dystrophic neurites of senile plaques (D). Paraffin sections without haematoxylin counterstaining, bar = 25 μm

DISCUSSION

This study shows altered mRNA expression and protein levels of crucial players in the process of protein synthesis, from the nucleolus to the ribosomes, in the DG and CA1 region of the hippocampus of AD cases at different stages of disease progression when compared with MA individuals with no neurological alterations and no AD-related pathology.

Nucleolar alterations

NCL, NPM1/B23 and NPM3 are major nucleolar proteins acting as histone-binding chaperones required for chromatin compacting and regulation of rRNA transcription (2, 18, 33, 37, 40, 41, 53, 65, 72, 74, 77, 97, 102, 104). NPM1 interacts with histones H3 and H4, and it is capable of nucleic acid binding (31, 77, 98). NPM1 is also involved in chromatin de-condensation, post-translational modification of histones, and nuclear re-programming (98). In addition, NPM1 is involved in the nuclear transport of proteins to the nucleolus and certain ribosomal proteins to the cytoplasm (6, 95, 96, 109). Additional functions of NPM1 are related to DNA replication, ribosome biogenesis, transcription, and repair (65). UBF encoded by *UBTF* (upstream binding transcription factor, RNA polymerase I gene) is associated with NOR and is required for rDNA transcription by RNA polymerase 1 (83). It is known that altered expression of nucleolar chaperones and factors involved in rRNA synthesis results in nucleolar stress which in turn leads to impaired ribosomal biogenesis (4, 58, 69, 79). The present observations show nucleolar stress in the hippocampus, mainly in CA1 but also in DG, in AD. Importantly, altered *NPM1* and *UBTF* gene expression is already observed in CA1 at stages I–II. Reduced NPM1, NPM3, NCL and UBF protein levels are seen in CA1 at stages III–IV (Tables 1 and 2). Therefore, nucleolar alterations in AD are probably not a mere consequence of cell death as altered mRNA regulation of *NPM1*

Table 3. mRNA expression of ribosomal proteins in the DG and CA1 region of the hippocampus of MA and AD cases.

Probe	MA	AD I–II	AD III–IV	AD V–VI	MA vs. AD I–II	MA vs. AD III–IV	MA vs. AD V–VI
DG							
RPL5	1.02 ± 0.23	0.94 ± 0.16	0.95 ± 0.19	0.97 ± 0.21	NS	NS	NS
RPL7	1.02 ± 0.22	0.91 ± 0.34	1.05 ± 0.26	0.41 ± 0.07	NS	NS	***↓
RPL21	1.02 ± 0,23	0.71 ± 0.38	0.80 ± 0.08	0.31 ± 0.08	NS	*↓	***↓
RPL22	1.07 ± 0.44	0.92 ± 0.43	0.92 ± 0.22	1.55 ± 0.12	NS	NS	*↑
RPL23A	1.02 ± 0.24	0.61 ± 0.24	0.76 ± 0.22	0.81 ± 0.15	*↓	*↓	NS
RPL26	1.07 ± 0.41	0.64 ± 0.32	0.74 ± 0.30	0.50 ± 0.24	*↓	NS	**↓
RPL27	1.03 ± 0.29	0.70 ± 0.26	0.75 ± 0.16	0.34 ± 0.09	NS	*↓	***↓
RPL30	1.07 ± 0.43	0.70 ± 0.08	0.77 ± 0.18	0.96 ± 0.29	NS	NS	NS
RPL31	1.03 ± 0.27	0.64 ± 0.25	0.83 ± 0.22	0.54 ± 0.14	*↓	NS	***↓
RPS3A	1.04 ± 0.30	0.98 ± 0.04	0.96 ± 0.19	0.96 ± 0.15	NS	NS	NS
RPS5	1.01 ± 0.20	0.66 ± 0.15	0.76 ± 0.14	0.96 ± 0.32	*↓	*↓	NS
RPS6	1.00 ± 0.11	0.80 ± 0.17	0.82 ± 0.18	0.88 ± 0.21	*↓	*↓	NS
RPS10	1.01 ± 0.19	0.65 ± 0.08	0.74 ± 0.13	0.62 ± 0.10	**↓	**↓	***↓
RPS13	1.02 ± 0.22	0.78 ± 0.39	0.75 ± 0.12	0.79 ± 0.10	*↓	*↓	NS
RPS16	1.03 ± 0.31	0.79 ± 0.39	0.72 ± 0.30	0.68 ± 0.26	NS	NS	*↓
RPS17	1.01 ± 0.14	0.82 ± 0.15	0.93 ± 0.20	0.48 ± 0.09	NS	NS	***↓
CA1							
RPL5	1.02 ± 0.23	1.33 ± 0.07	1.27 ± 0.15	1.33 ± 0.25	**↑	*↑	*↑
RPL7	1.04 ± 0.31	1.28 ± 0.20	1.30 ± 0.13	0.78 ± 0.12	NS	NS	NS
RPL21	1.04 ± 0.33	0.91 ± 0.30	0.79 ± 0.11	0.41 ± 0.25	NS	NS	***↓
RPL22	1.07 ± 0.48	0.84 ± 0.15	0.88 ± 0.21	0.70 ± 0.08	NS	NS	NS
RPL23A	1.04 ± 0.31	0.78 ± 0.26	0.67 ± 0.15	0.59 ± 0.08	NS	**↓	**↓
RPL26	1.09 ± 0.46	1.60 ± 0.19	1.14 ± 0.40	0.53 ± 0.21	*↑	NS	*↓
RPL27	1.04 ± 0.33	0.86 ± 0.21	1.06 ± 0.15	1.05 ± 0.15	NS	NS	NS
RPL30	1.03 ± 0.27	0.81 ± 0.21	1.12 ± 0.32	1.70 ± 0.29	NS	NS	***↑
RPL31	1.04 ± 0.33	0.90 ± 0.12	1.09 ± 0.19	0.55 ± 0.16	NS	NS	**↓
RPS3A	1.06 ± 0.40	0.96 ± 0.11	1.24 ± 0.13	1.05 ± 0.23	NS	NS	NS
RPS5	1.04 ± 0.29	0.75 ± 0.18	0.81 ± 0.14	0.89 ± 0.10	*↓	*↓	NS
RPS6	1.06 ± 0.36	0.66 ± 0.20	0.84 ± 0.12	0.49 ± 0.08	*↓	NS	***↓
RPS10	1.05 ± 0.34	0.84 ± 0.16	0.98 ± 0.17	0.65 ± 0.13	NS	NS	*↓
RPS13	1.04 ± 0.30	1.01 ± 0.21	1.19 ± 0.22	0.17 ± 0.04	NS	NS	***↓
RPS16	1.08 ± 0.38	0.97 ± 0.25	1.01 ± 0.59	0.09 ± 0.03	NS	NS	*↓
RPS17	1.01 ± 0.14	0.98 ± 0.19	1.11 ± 0.23	0.26 ± 0.05	NS	NS	*↓

Expression levels are calculated using Gus-β for normalization; Student *t*-test *$P < 0.05$; **$P < 0.01$; ***$P < 0.001$ compared with MA.

and *UBTF* first occurs before any evidence of neuron loss in the CA1 region of the hippocampus at stages I–II. Lack of perfect match between mRNA levels and corresponding proteins, as seen in relation with increased *NPM1* and *NPM3* mRNAs and decreased NPM1 and NPM3 protein levels in the CA1 region of the hippocampus at stages III–IV, is not rare in human neurodegenerative diseases and can be explained by the concomitant activity of epigenetic factors as several types of non-coding RNAs. Reduced numbers of nucleoli as revealed with Nissl staining together with significant decreased numbers of NPM1-, NPM3-, NCL- and UBF-immunoreactive nucleoli is consistent, in part, with neuron loss at stages III–IV and V–VI. In addition, immunohistochemistry shows reduced immunoreactivity in remaining nucleoli at middle and advanced stages of the disease thus suggesting declining immunoreactivity in surviving cells.

Nucleolar alterations in AD are accompanied by altered regulation of rRNA expression. Thus, 28S rRNA in CA1 is down-regulated at stages I–IV and up-regulated at stages V–VI compared with MA and 28S rRNA in the DG is transiently down-regulated at stages III–IV in AD. As alterations of NCL, NPMs and UBF increase with disease progression whereas alterations of rRNA vary along disease, other factors, as epigenetic regulation of rDNA (80), are probably implicated in the altered rRNA biogenesis in AD. In this line, it is particularly intriguing and unresolved the increased expression levels of 28S rRNA in the CA1 region at advanced stages of AD and the transient decrease of 28S rRNA in DG. However, it is well known that oxidative damage to mRNA, tRNA and rRNA occurs in AD and that such damage may produce ribosomal dysfunction and altered protein synthesis (26, 27, 48, 75, 76, 90, 91). As a working hypothesis, it can be postulated that oxidative damage to RNA triggers epigenetic responses which in turn modulate by activation or by repression the expression of variegated molecules implicated in ribosomal biogenesis.

Nuclear alterations

Regarding the nucleus, NCL and NPMs regulate rRNA transcription through the modulation of H3K9m2 and H4K12ac in rRNA genes (18, 98). H3K9me2 and H4K12ac nuclear immunoreactivity declines in CA1 and DG with AD progression thus suggesting that specific post-translational modifications of selected histones which

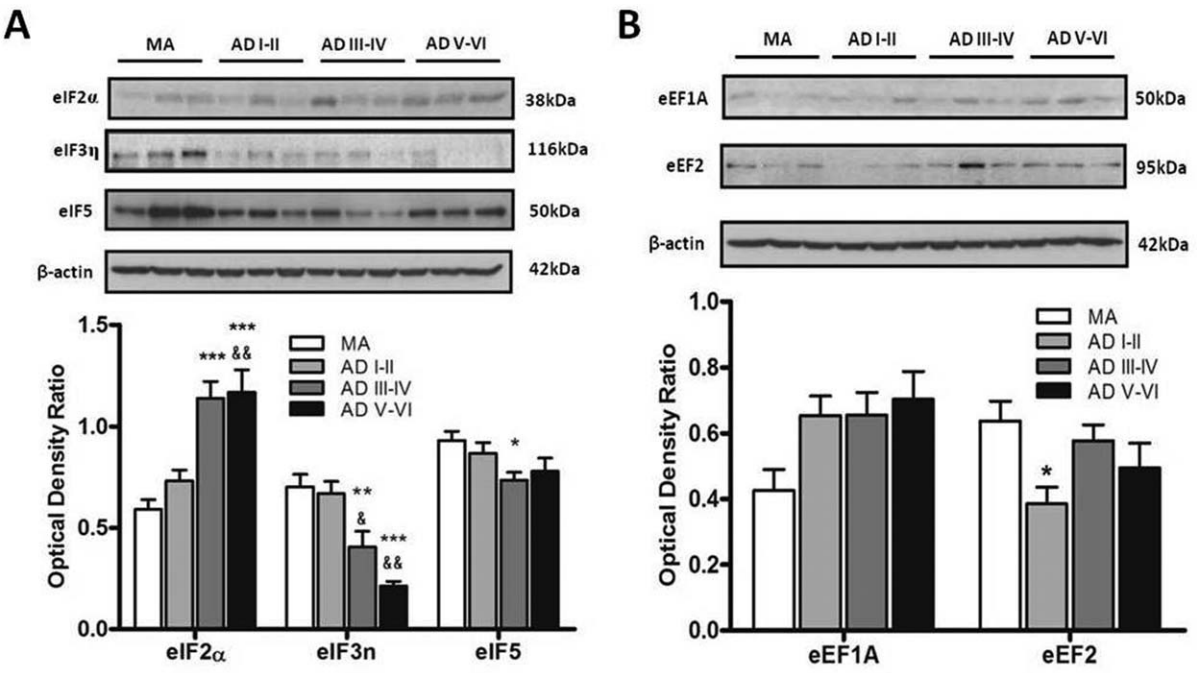

Figure 5. Eukaryotic translation factors in the CA1 region of MA and AD cases. **A.** Representative western blots and densitometric analysis of the content of eIF2 α, eIF3η, eiF5 in the CA1 region of MA, AD I–II, AD III–IV, and AD V–VI cases. **B.** Western blot analysis of eEF1A and eEF2 in the CA1 region of MA, AD I–II, AD III–IV, and AD V–VI cases. β-actin levels are used to normalize total protein content. The values represent the mean $\pm$ standard error of the mean (SEM) of 6–7 cases for group. $^{*}P > 0.05$, $^{**}P > 0.01$ compared with MA.

are involved in rRNA synthesis are altered in hippocampus neurons in AD.

Protein tau is localized in the nucleus of neuroblastoma cells (44, 45, 66, 100, 105), non-neural cells (21, 68, 101), and neurons in human brain (14). Tau binds to double- and single-strands of DNA *in vitro* (51, 61, 78) and both the proline-rich domain and the microtubule-binding domain of tau are known to contribute to its interaction with DNA (107). Nuclear tau induces DNA conformational changes in neural cells (81), protects DNA from denaturation *in vitro* (51, 52), prevents DNA damage by oxidative stress (94, 106), and confers stability to DNA (15, 92). Histone deacetylase 6 interacts with the microtubule-associated protein tau (25).The present data illustrate a marked decrease of nuclear tau-100 in CA1 and DG neurons with disease progression. Nuclear tau-100 virtually disappears in neurons with NFTs. This is a very important point as it has been postulated that tau promotes neurodegeneration through global chromatin relaxation in AD because increased tau hyperphosphorylation and tangle formation in the cytoplasm parallels chromatin disassembly (39). Although such explanation may be correct, the present findings offer an additional scenario: tau accumulation in NFTs is only one of the terminal stages of tau metabolism disruption in AD. Decreased levels of nuclear tau precede cytoplasmic tau hyper-phosphorylation. Moreover, decreased nuclear tau is not restricted to neurons with NFTs. Therefore, reduced nuclear tau is a distinct alteration of tau metabolism in AD. As a working hypothesis, it can be suggested that it is not the accumulation of cytoplasmic hyper-phosphorylated tau which disassembles chromatin but rather it is the decrease in nuclear tau that is responsible for DNA disassembly. Eventually, nuclear tau is no longer present in neurons with NFTs. The relationship between reduced nuclear tau, histone modifications and chromatin relaxation is, at present, under study.

Altered ribosomes

Ribosomes are composed of 65% RNAs and 35% ribosomal proteins that form the small subunit (40S) which binds to mRNA and the large subunit (60S) which binds to tRNAs and amino acids. In eukaryotes, the small subunit is made of 18S rRNA and 33 proteins whereas the larger subunit consists of 5S rRNA, 5.8S rRNA, 28S rRNA, and 46 ribosomal proteins (19, 29, 30, 38, 42, 43, 46, 59, 60, 93, 108). Eleven of sixteen mRNAs encoding ribosomal proteins examined here are altered in CA1 in AD at stage V–VI, and nine of sixteen in the DG at the same AD stage. It can be suggested that down-regulation of ribosomal protein genes is the result of neuron loss at advanced stages of the disease, but 3 RPLs and 4 RPSs are down-regulated in the DG and two RPLs and two RPSs are up- and down-regulated, respectively in CA1 in AD stages I–II of Braak and Braak. Therefore, altered gene expression of ribosomal proteins occurs before the appearance of cell death. Nucleolar stress, a well-known disturbing factor of ribosomal biogenesis (71), can be considered as a putative inducing factor of altered ribosomal gene expression at early stages of AD.

Altered expression of factors involved in protein biosynthesis

Translation initiation in the ribosome is geared by the interactions of 12 eukaryotic translation initiation factors (eIFs), most of them composed of several subunits (55, 57). Elongation occurs when elongating factor eEF1A is activated following GTP binding and

forms a complex with aminoacyl-tRNA which recognizes the specific sequence in mRNA at the ribosome. Once the interaction of the codon in mRNA with the anti-codon in tRNA is decoded, eEF1A-GDP is hydrolysed, released from the ribosome, and recycled into its active form by eEF1B. eEF2 assists in the precise codon location at the ribosome (1, 24, 70, 73, 85, 103).eIF3η and eIF5 protein levels are reduced whereas eIF2α protein levels are increased in the CA1 region of the hippocampus in AD with disease progression. Increased eIF2α correlates with increased p-eIF2α in AD as previously reported (17, 34, 49, 50). Phosphorylation of eIF2 on its α subunit prevents the delivery of initiator methionyl-tRNA, resulting in global inhibition of translation of most mRNAs (47). Together these observations support altered protein synthesis with disease progression.

Final comments

Several studies have shown altered gene expression in the post-mortem brain of cases with AD and related animal models (7, 67, 99). However, this is the first study showing altered pathways related to protein synthesis including altered mRNA and protein expression of certain nucleolar chaperones, factors linked to DNA polymerases, altered methylation and acetylation of specific histones, altered expression of nuclear tau, abnormal rRNA expression, altered expression of several *RPL* and *RPS* genes, and altered expression of certain initiation and elongation factors of protein synthesis at the ribosome in the AD hippocampus.

It can be argued that none of these alterations proves that protein synthesis is impaired in AD. However, analysis of protein synthesis using incorporation of labeled amino acids to proteins in post-mortem human brain samples has been unsuccessful. Very low and erratic incorporation of S^{35} methionine into protein has made impossible to replicate previous experiments performed by other authors (26, 27).

As mentioned in previous paragraphs, not all these changes can be linked to neuronal loss as they first appear at stages in which no cell death is found in the hippocampus in AD. It is worth stressing that the expression of *NPM1* and *UBTF* mRNAs, 28sRNA, *RPL5*, *RPL26*, *RPS5* and *RPS6* mRNAs, and eEF2 protein is altered in the CA1 at stages I–II of Braak and Braak. *RPL23A*, *RPL26*, *RPL31*, *RPS5*, *RPS6*, *RPS10* and *RPS13* mRNAs are down-regulated in DG at stages I–II. Therefore, the present findings show also for the first time that multiple alterations in pathways involved in protein synthesis occur at very early stages of cases with AD-related pathology, before the appearance of clinical symptoms if they would ever have appeared (35). Finally, it is important to note that changes in AD differ in the CA1 and DG at the beginning and along disease progression. The reason of regional vulnerability in neurodegenerative diseases is a long-lasting non-solved question that is the subject of continuous attention.

Progressive atrophy of the hippocampus, as visualized with several neuroimaging techniques and in a particular clinical context, is currently used as a biomarker of AD progression (8). This change has been mainly interpreted as being the result of loss of afferents to the DG and to the loss of neurons in the CA1 region of the hippocampus (107). However, morphological and immunohistochemical studies have shown reduced dendritic arbors, reduced numbers of synapses, and reduced synaptic protein markers both in the CA1 region of the hippocampus and in the DG (32, 36, 56, 82, 86–89). The present observations may help to improve understanding of neuronal atrophy in CA1 and DG in AD resulting from altered molecular machinery of protein synthesis involving specific pathways in the nucleolus, nucleus and ribosome.

ACKNOWLEDGMENTS

The authors thank Margarita Carmona for technical assistance and Tom Yohannan for editorial help. This study was funded by the Seventh Framework Programme of the European Commission, grant agreement 278486: DEVELAGE and the Ministerio de Ciencia e Innovación, Instituto de Salud Carlos III–Fondos FEDER, a way to build Europe FIS PIE14/00034 and PI14/00757.

REFERENCES

1. Andersen GR, Nissen P, Nyborg J (2003) Elongation factors in protein biosynthesis. *Trends Biochem Sci* **28**:434–441.
2. Angelov D, Bondarenko VA, Almagro S, Menoni H, Mongelard F, Hans F *et al* (2006) Nucleolin is a histone chaperone with FACT like activity and assists remodeling of nucleosomes. *EMBO J* **25**:1669–1679.
3. Apostolova LG, Dutton Ra, Dinov ID, Hayashi KM, Toga AW, Cummings JL, Thompson PM (2006) Conversion of mild cognitive impairment to Alzheimer disease predicted by hippocampal atrophy maps. *Arch Neurol* **63**:693–699.
4. Avitabile D, Bailey B, Cottage CT, Sundararaman B, Joyo A, McGregor M *et al* (2011) Nucleolar stress is an early response to myocardial damage involving nucleolar proteins nucleostemin and nucleophosmin. *Proc Natl Acad Sci USA* **108**:6145–6150.
5. Barnes J, Bartlett J, van de Pol L, Loy C, Scahill RI, Frost C *et al* (2009) A meta-analysis of hippocampal atrophy rates in Alzheimer's disease. *Neurobiol Aging* **30**:1711–1723.
6. Borer RA, Lehner CF, Eppenberger HM, Nigg EA (1989) Major nucleolar proteins shuttle between nucleus and cytoplasm. *Cell* **56**:379–390.
7. Bossers K, Wirz KT, Meerhoff GF, Essing AH, van Dongen JW, Houba P *et al* (2010) Concerted changes in transcripts in the prefrontal cortex precede neuropathology in Alzheimer's disease. *Brain* **133**:3699–3723.
8. Boutet C, Chupin M, Lehéricy S, Marrakchi-Kacem L, Epelbaum S, Poupon C *et al* (2014) Detection of volume loss in hippocampal layers in Alzheimer's disease using 7 T MRI: a feasibility study. *Neuroimage Clin* **5**:341–348.
9. Braak H, Alafuzoff I, Arzberger T, Kretzschmar H, Del Tredici K (2006) Staging of Alzheimer disease-associated neurofibrillary pathology using paraffin sections and immunocytochemistry. *Acta Neuropathol* **12**:389–404.
10. Braak H, Braak E (1991) Neuropathological staging of Alzheimer-related changes. *Acta Neuropathol* **82**:239–259.
11. Braak H, Braak E (1997) Frequency of stages of Alzheimer-related lesions in different age categories. *Neurobiol Aging* **18**:351–357.
12. Braak H, Braak E (1999) Temporal sequence of Alzheimer's disease-related pathology. In: *Cerebral Cortex* vol. 14, Neurodegenerative and Age-Related Changes in Structure and Function of Cerebral Cortex. A Peters, JH Morrison (eds), pp. 475–512. Kluwer Academic/Plenum Publishers: New York, Boston, Dordrecht, London, Moscow.
13. Braak H, Thal DR, Ghebremedhin E, del Tredici K (2011) Stages of the pathologic process in Alzheimer disease: age categories from 1 to 100 years. *J Neuropathol Exp Neurol* **70**:960–969.
14. Brady RM, Zinkowski RP, Binder LI (1995) Presence of tau in isolated nuclei from human brain. *Neurobiol Aging* **16**:479–486.

15. Brady RM, Zinkowski RP, Binder LI. Camero S, Benítez MJ, Barrantes A *et al* (2014) Tau protein provides DNA with thermodynamic and structural features which are similar to those found in histone-DNA complex. *J Alzheimers Dis* **39**:649–660.
16. Csernansky JG, Wang L, Swank J, Miller JP, Gado M, McKeel D *et al* (2005) Preclinical detection of Alzheimer's disease: hippocampal shape and volume predict dementia onset in the elderly. *Neuroimage* **25**:783–792.
17. Chang RC, Wong AK, Ng HK, Hugon J (2002) Phosphorylation of eukaryotic initiation factor-2alpha (eIF2alpha) is associated with neuronal degeneration in Alzheimer's disease. *Neuroreport* **13**:2429–2432.
18. Cong R, Das S, Ugrinova I, Kumar S, Mongerlard F, Wong J, Bouvet P (2012) Interaction of nucleolin with ribosomal RNA genes and its role in RNA polymerase I transcription. *Nucleic Acids Res* **40**:9441–9454.
19. Connell SR, Trieber CA, Stelzl U, Einfeldt E, Taylor DE, Nierhaus KH (2002) The tetracycline resistance protein Tet(o) perturbs the conformation of the ribosomal decoding centre. *Mol Microbiol* **45**: 1463–1472.
20. Convit A, De Leon M, Tarshish C, De Santi S, Tsui W, Rusinek H, George A (1997) Specific hippocampal volume reductions in individuals at risk for Alzheimer's disease. *Neurobiol Aging* **18**:131–138.
21. Cross DC, Muñoz JP, Hernández P, Maccioni RB (2000) Nuclear and cytoplasmic tau proteins from human non-neuronal cells share common structural and functional features with brain tau. *J Cell Biochem* **78**:305–317.
22. da Silva AM, Payão SL, Borsatto B, Bertolucci PH, Smith MA (2000) Quantitative evaluation of rRNA in Alzheimer's disease. *Mech Ageing Dev* **120**:57–64.
23. De Leon MJ, DeSanti S, Zinkowski R, Mehta PD, Pratico D, Segal S *et al* (2006) Longitudinal CSF and MRI biomarkers improve the diagnosis of mild cognitive impairment. *Neurobiol Aging* **27**: 394–401.
24. Dever TE, Green R (2012) The elongation, termination, and recycling phases of translation in eukaryotes. *Cold Spring Harb Perspect Biol* **4**:a013706.
25. Ding H, Dolan PJ, Johnson GV (2008) Histone deacetylase 6 interacts with the microtubule-associated protein tau. *J Neurochem* **106**:2119–2130.
26. Ding Q, Markesbery WR, Chen Q, Li F, N. Keller JN (2005) Ribosome dysfunction is an early event in Alzheimer's disease. *J Neurosci* **25**:9171–9175.
27. Ding Q, Markesbery WR, Cecarini V, Keller JN (2006) Decreased RNA, and increased RNA oxidation, in ribosomes from early Alzheimer's disease. *Neurochem Res* **31**:705–710.
28. Dönmez-Altuntas H, Akalain H, Karaman Y, Demirtas H, Imamoglu N, Ozkul Y (2005) Evaluation of the nucleolar organizer regions in Alzheimer's disease. *Gerontology* **51**:297–301.
29. Doudna JA, Rath VL (2002) Structure and function of the eukaryotic ribosome: the next frontier. *Cell* **109**:153–156.
30. Dresios J, Panopoulos P, Synetos D (2006) Eukaryotic ribosomal proteins lacking a eubacterial counterpart: important players in ribosomal function. *Mol Microbiol* **59**:1651–1663.
31. Dumbar TS, Gentry GA, Olson MOJ (1989) Interaction of nucleolar phosphoprotein B23 with nucleic acids. *Biochemistry* **28**:9495–9501.
32. Einstein G, Buranosky R, Crain BJ (1994) Dendritic pathology of granule cells in Alzheimer's disease is unrelated to neuritic plaques. *J Neurosci* **14**:5077–5088.
33. Erard MS, Belenguer P, Caizergues-Ferrer M, Pantaloni A, Amalric F (1988) A major nucleolar protein, nucleolin, induces chromatin decondensation by binding to histone H1. *Eur J Biochem* **175**:525–530.
34. Ferrer I (2002) Differential expression of phosphorylated translation initiation factor 2 alpha in Alzheimer's disease and Creutzfeldt-Jakob's disease. *Neuropathol Appl Neurobiol* **28**:441–451.
35. Ferrer I (2012) Defining Alzheimer as a common age-related neurodegenerative process not inevitably leading to dementia. *Prog Neurobiol* **97**:38–51.
36. Flood DG, Coleman PD (1986) Failed compensatory dendritic growth as a pathophysiological process in Alzheimer's disease. *Can J Neurol Sci* **13**(Suppl. 4):475–479.
37. Frehlick LJ, Eirín-López JM, Ausio J (2007) New insights into the nucleophosmin/nucleoplasmin family of nuclear chaperones. *Bioassays* **29**:49–59.
38. Fromont-Racine M, Senger B, Saveanu C, Fasiolo F (2003) Ribosome assembly in eukaryotes. *Gene* **313**:17–42.
39. Frost B, Hemberg M, Lewis J, Freany MB (2014) Tau promotes neurodegeneration through global chromatin relaxation. *Nature Neurosci* **17**:357–366.
40. Gadad SS, Shandilya J, Kishore AH, Kundu TK (2010) NPM3, a member of the nucleoiphosmin/nucleoplasmin family, enhances activator-dependent transcription. *Biochemistry* **49**:1355–1357.
41. Ginisty H, Sicard H, Roger B, Bouvet P (1999) Structure and functions of nucleolin. *J Cell Sci* **112**:761–772.
42. Glück A, Wool IG (2002) Analysis by systematic deletion of amino acids of the action of the ribotoxin restrictocin. *Biochim Biophys Acta* **1594**:115–126.
43. Granneman S, Baserga SJ (2004) Ribosome biogenesis: of knobs and RNA processing. *Exp Cell Res* **296**:43–50.
44. Greenwood JA, Johnson GWW (1995) Localization and *in situ* phosphorylation state of nuclear tau. *Exp Cell Res* **220**:332–337.
45. Haque N, Tanaka T, Iqbal K, Grundke-Iqbal I (1999) Regulation of expression, phosphorylation and biological activity of tau during differentiation in SY5Y cells. *Brain Res* **838**:69–77.
46. Henras AK, Soudet J, Gérus M, Lebaron S, Caizergues-Ferrer M, Mougin A, Henry Y (2008) The post-transcriptional steps of eukaryotic ribosome biogenesis. *Cell Mol Life Sci* **65**:2334–2359.
47. Harding HP, Zhang Y, Ron D (1999) Protein translation and folding are coupled by an endoplasmic-reticulum-resident kinase. *Nature* **397**: 271–274.
48. Honda K, Smith MA, Zhu X, Baus D, Merrick WC, Tartakoff AM *et al* (2005) Ribosomal RNA in Alzheimer disease is oxidized by bound redox-active iron. *J Biol Chem* **280**:20978–20986.
49. Hoozemans JJ, van Haastert ES, Nijholt DA, Rozemuller AJ, Eikelenboom P, Scheper W (2009) The unfolded protein response is activated in pretangle neurons in Alzheimer's disease hippocampus. *Am J Pathol* **174**:1241–1251.
50. Hoozemans JJ, Veerhuis R, Van Haastert ES, Rozemuller JM, Baas F, Eikelenboom P, Scheper W (2005) The unfolded protein response is activated in Alzheimer's disease. *Acta Neuropathol* **110**:165–172.
51. Hua Q, He RQ, Haque N, Qu MH, del Carmen Alonso A, Grundke-Iqbal I, Iqbal K (2003) Microtubule associated protein tau binds to double-stranded but not single-stranded DNA. *Cell Mol Life Sci* **60**: 413–421.
52. Hua Q, He R (2005) Tau could protect DNA double helix structure. *Biochem Biophys Acta* **1645**:205–211.
53. Huang N, Negi S, Szebeni A, Olson MOJ (2005) Protein NPM3 interacts with the multifunctional nucleolar protein B23/ nucleophosmin and inhibits ribosome biogenesis. *J Biol Chem* **280**: 5496–5502.
54. Jack CR, Petersen RC, Xu CY, Waring SC, Brien PCO, Tangalos EG *et al* (1997) Medial temporal atrophy on MRI in normal aging and very mild Alzheimer's disease. *Neurology* **49**:786–794.
55. Jackson RJ, Hellen CU, Pestova TV (2010) The mechanism of eukaryotic translation initiation and principles of its regulation. *Nat Rev Mol Cell Biol* **11**:113–127.

56. Kaufmann WA, Barnas U, Humpel C, Nowakowski K, DeCol C, Gurka P *et al* (1998) Synaptic loss reflected by secretoneurin-like immunoreactivity in the human hippocampus in Alzheimer's disease. *Eur J Neurosci* **10**:1084–1094.
57. Kapp LD, Lorsch JR (2004) The molecular mechanisms of eukaryotic translation. *Annu Rev Biochem* **73**:657–704.
58. Kiryk A, Sowodniok K, Kreiner G, Rodriguez-Parkitna J, Sönmez A, Górkiewicz T *et al* (2013) Impaired rRNA synthesis triggers homeostatic responses in hippocampal neurons. *Front Cell Neurosci* **7**:207.
59. Klein DJ, Moore PB, Steitz TA (2004) The roles of ribosomal proteins in the structure assembly, and evolution of the large ribosomal subunit. *J Mol Biol* **340**:141–177.
60. Korobeinikova AV, Garber MB, Gongadze GM (2012) Ribosomal proteins: structure, function, and evolution. *Biochemistry* **77**:562–574.
61. Krylova SM, Musheev M, Nutiu R, Li Y, Lee G, Krylov SN (2005) Tau protein binds single-stranded DNA sequence specifically: the proof obtained in vitro with non-equilibrium capillary electrophoresis of equilibrium mixtures *FEBS Lett* **579**:1371–1375.
62. Langstrom NS, Anderson JP, Lindroos HG, Winblad B, Wallace WC (1989) Alzheimer's disease-associated reduction of polysomal mRNA translation. *Brain Res Mol Brain Res* **5**:259–269.
63. Li YD, Dong HB, Xie GM, Zhang LJ (2013) Discriminative analysis of mild Alzheimer's disease and normal aging using volume of hippocampal subfields and hippocampal mean diffusivity: an in vivo magnetic resonance imaging study. *Am J Alzheimers Dis Other Demen* **28**:627–633.
64. Li X, An WL, Alafuzoff I, Soininen H, Winblad B, Pei JJ (2004) Phosphorylated eukaryotic translation factor 4E is elevated in Alzheimer brain. *Neuroreport* **15**:2237–2240.
65. Lindström MS (2011) NPM1/B23: a multifunctional chaperone in ribosome biogenesis and chromatin remodeling. *Biochem Res Int* **2011**: 195209.
66. Loomis PA, Howard TH, Castleberry RP, Binder LI (1990) Identification of nuclear tau isoforms in human neuroblastoma cells. *Proc Natl Acad Sci USA* **87**:8422–8426.
67. López-González I, Schlüter A, Aso E, Garcia-Esparcia P, Ansoleaga B, LLorens F *et al* (2015) Neuroinflammatory signals in Alzheimer disease and APP/PS1 transgenic mice: correlations with plaques, tangles, and oligomeric species. *J Neuropathol Exp Neurol* **74**: 319–344.
68. Lu Q, Wood JG (1993) Characterisation of fluorescently derivatized bovine tau protein and its localization and functions in cultured Chinese hamster ovary cells. *Cell Motil Cytoskeleton* **25**:190–200.
69. McKeown PC, Shaw PJ (2009) Chromatin: linking structure and function in the nucleolus. *Chromosoma* **118**:11–23.
70. Merrick WC, Nyborg J (2000) The protein biosynthesis elongation cycle. In: *Translational Control of Gene Expression*, N Sonenberg, JWB Hershey, MB Mathews (eds), pp. 89–125. Cold Spring Harbor Laboratory Press: New York.
71. Montanaro L, Treré D, Derenzini M (2008) Nucleolus, ribosomes, and cancer. *Am J Pathol* **173**:301–310.
72. Motoi N, Suzuki K, Hirota R Johnson P, Oofusa K, Kikuchi Y, Yoshizato K (2008) Identification and characterization of nucleoplasmin 3 as a histone-binding protein in embryonic stem cells. *Dev Growth Diff* **50**:307–320.
73. Nakamura Y, Ito K (2011) tRNA mimicry in translation termination and beyond. *Wiley Interdiscip Rev RNA* **2**:647–668.
74. Namboodiri VMH, Akey IV, Schmidt-Zachmann MS, Head JF, Akey CW (2004) The structure and function of Xenopus NO38-core, a histone chaperone in the nucleolus. *Structure* **12**:2149–2160.
75. Nunomura A, Chiba S, Lippa CF, Cras P, Kalaria RN, Takeda A *et al* (2004) Neuronal RNA oxidation is a prominent feature of familial Alzheimer's disease. *Neurobiol Dis* **17**:108–113.
76. Nunomura A, Honda K, Takeda A, Hirai K, Zhu X, Smith MA, Perry G (2006) Oxidative damage to RNA in neurodegenerative diseases. *J Biomed Biotechnol* **2006**:82323.
77. Okuwaki M, Matsumoto K, Tsujimoto M, Nagata K (2011) Function of nucleoplasmin/B23, a nucleolar acidic protein, a s a histone chaperone. *FEBS Lett* **506**:272–276.
78. Padmaraju V, Indi SS, Rao JSJ (2010) New evidences on tau-DNA interactions and relevance to neurodegeneration. *Neurochem Int* **57**: 51–57.
79. Parlato R, Kreiner G (2013) Nucleolar activity in neurodegenerative diseases: a missing piece of the puzzle? *J Mol Med* **91**:541–547.
80. Pietrzak M, Rempala G, Nelson PT, Zheng JJ, Hetman M (2011) Epigenetic silencing of nucleolar rRNA genes in Alzheimer's disease *PLoS One* **6**:e22585.
81. Qu MH, Li H, Tian R, Nie CL, Liu Y Han BS, He RQ (2004) Neuronal tau induces DNA conformational changes observed by atomic force microscopy. *Neuroreport* **15**:2723–2727.
82. Robinson JL, Molina-Porcel L, Corrada MM, Raible K, Lee EB, Lee VM *et al* (2014) Perforant path synaptic loss correlates with cognitive impairment and Alzheimer's disease in the oldest-old. *Brain* **137**: 2578–2587.
83. Roussel P, André C, Masson C, Géraud G, Hernandez-Verdun D (1993) Localization of the RNA polymerase I transcription factor hUBF during the cell cycle. *J Cell Sci* **104**:327–337.
84. Sajdel-Sulkowska EM, Marotta CA (1984) Alzheimer's disease brain: alterations in RNA levels and in a ribonuclease-inhibitor complex. *Science* **225**:947–949.
85. Sasikumar AN, Perez WB, Kinzy TG (2012) The many roles of the eukaryotic elongation factor 1 complex. *Wiley Interdiscip Rev RNA* **3**: 543–555.
86. Scheff SW, Price DA (1998) Synaptic density in the inner molecular layer of the hippocampal dentate gyrus in Alzheimer disease. *J Neuropathol Exp Neurol* **57**:1146–1153.
87. Scheff SW, Price DA (2003) Synaptic pathology in Alzheimer's disease: a review of ultrastructural studies. *Neurobiol Aging* **24**:1029–1046.
88. Scheff SW, Price DA (2006) Alzheimer's disease-related alterations in synaptic density: neocortex and hippocampus. *J Alzheimers Dis* **9**(Suppl 3):101–115.
89. Scheff SW, Price DA, Schmitt FA, Mufson EJ (2006) Hippocampal synaptic loss in early Alzheimer's disease and mild cognitive impairment. *Neurobiol Aging* **27**:1372–1384.
90. Shan X, Lin CL (2006) Quantification of oxidized RNAs in Alzheimer's disease. *Neurobiol Aging* **27**:657–662.
91. Shan X, Tashiro H, Lin CL (2003) The identification and characterization of oxidized RNAs in Alzheimer's disease. *J Neurosci* **23**:4913–4921.
92. Sjöberg MK, Shestakova E, Mansuroglu Z, Maccioni RB, Bonnefoy E (2006) Tau protein binds to peri-centromeric DNA: a putative role for nuclear tau in nucleolar organization. *J Cell Sci* **119**: 2025–2034.
93. Stelzl U, Connell S, Nierhaus KH, Wittmann-Liebold B (2001) Ribosomal proteins: role in ribosomal function. *Encyclopedia Life Sci*: 1–12.
94. Sultan A, Nesslany F, Violet M, Bégard S, Loyens A, Talahari S *et al* (2011) Nuclear tau, a key player in neuronal DNA protection. *J Biol Chem* **286**:4566–4575.
95. Szebeni A, Herrera JE, Olson MOJ (1995) Interaction of nucleolar protein B23 with peptides related to nuclear localization signals. *Biochemistry* **34**:8037–8042.
96. Szebeni A, Mehrotra B, Baumann A, Adam SA, Wingfield PT, Olson MOJ (1997) Nucleolar protein B23 stimulate nuclear import of the HIV-1 Rev protein and NLS-conjugated albumin. *Biochemistry* **36**: 3941–3949.

97. Tajrishi MM, Tuteja R, Tuteja N (2011) The most abundant multifunctional phosphoprotein of nucleolus. *Commun Integr Biol* **4**: 267–275.
98. Tamada H, Thuan NV, Reed P, Nelson D, Katoku-Kikyo N, Wudel J *et al* (2006) Chromatin decondensation and nuclear reprogramming by nucleoplasmin. *Mol Cell Biol* **26**:1259–1271.
99. Tan MG, Chua WT, Esiri MM, Smith AD, Vinters HV, Lai MK (2010) Genome wide profiling of altered gene expression in the neocortex of Alzheimer's disease. *J Neurosci Res* **88**:1157–1169.
100. Thurston VC, Pena P, Pestell R, Binder L (1997). Nucleolar localization of the microtubule-associated protein tau in neuroblastomas using sense and anti-sense transfection strategies *Cell Motil Cytoskeleton* **38**:100–110.
101. Thurston VC, Zinkowski RP, Binder LI (1996) Tau as a nucleolar protein in human non-neural cells in vitro and in vivo. *Chromosoma* **105**:20–30.
102. Tuteja R, Tuteja N (1998) Nucleolin: a multifunctional major nucleolar phosphoprotein. *Clin Rev Biochem Mol Biol* **33**: 407–436.
103. Voorhees RM, Ramakrishnan V (2013) Structural basis of the translational elongation cycle. *Annu Rev Biochem* **82**:203–236.
104. Wang D, Baumann A, Szebeni A, Olson MOJ (1994) The nucleic acid binding activity of nucleolar protein B23.1 resiudes in its carboxyl-terminal end. *J Biol Chem* **269**:30994–30998.
105. Wang Y, Loomis PA, Zinkowski RP, Binder LI (1993) A novel tau transcript in cultured human neuroblastoma cells expressing nuclear tau. *J Cell Biol* **121**:257–267.
106. Wei Y, Qu MH, Wang Xs, Chen L, Wang DL, Liu Y *et al* (2008) Binding to the minor groove of the double-strand, tau protein prevents DNA from damage by peroxidation. *PLoS One* **3**:e2600.
107. West MJ, Kawas CH, Stewart WF, Rudow GL, Troncoso JC (2004) Hippocampal neurons in pre-clinical Alzheimer's disease. *Neurobiol Aging* **25**:1205–1212.
108. Wilson DN, Blaha G, Connell SR, Ivanov PV, Jenke H, Stelzl U *et al* (2002) Protein synthesis at atomic resolution: mechanistics of translation in the light of highly resolved structures for the ribosome. *Curr Protein Pept Sci* **3**:1–53.
109. Yu Y, Maggi LB, Brady SN, Apicelli AJ, Dai MS, Lu H, Weber JD (2006) Nucleophosmin is essential for ribosomal protein L5 nuclear export. *Mol Cell Biol* **26**:3798–3809.

SUPPORTING INFORMATION

Additional Supporting Information may be found in the online version of this article at the publisher's web-site:

Table I. Summary of cases and methods used in the present series. Age in years, p-m delay: post-mortem delay; MA: middle-aged without neurological and mental disease and no alterations in the neuropathological study, AD: Alzheimer's diseases stages of Braak and Braak; ih: immunohistochemistry, wb: western blotting.
Table II. TaqMan probes. Gene abbreviation, full name and sequence.
Table III. Characteristics of antibodies. rb: rabbit polyclonal, ms: mouse monoclonal, ih: immunohistochemistry, wb: western blotting.